





Type I IFN is siloed in endosomes

Jennie B. Altman^a, Justin Taft^a, Tim Wedeking^b, Conor N. Gruber^a, Michael Holtmannspötter^{b,c} , Jacob Piehler^{b,d} , and Dusan Bogunovic^{a,e,f,g,1}

^aDepartment of Microbiology, Icahn School of Medicine at Mount Sinai, New York, NY 10029; ^bDivision of Biophysics, Department of Biology, Osnabrück University, 49076 Osnabrück, Germany; ^cIntegrated Bioimaging Facility, Osnabrück University, 49076 Osnabrück, Germany; ^dCenter for Cellular Nanoanalytics, Osnabrück University, 49076 Osnabrück, Germany; ^eDepartment of Pediatrics, Icahn School of Medicine at Mount Sinai, New York, NY 10029; ^fPrecision Immunology Institute, Icahn School of Medicine at Mount Sinai, New York, NY 10029; and ^gMindich Child Health and Development Institute, Icahn School of Medicine at Mount Sinai, New York, NY 10029

Edited by Tak W. Mak, University of Toronto, Toronto, ON, Canada, and approved June 16, 2020 (received for review December 6, 2019)

Type I IFN (IFN-I) is thought to be rapidly internalized and degraded following binding to its receptor and initiation of signaling. However, many studies report the persistent effects mediated by IFN-I for days or even weeks, both ex vivo and in vivo. These long-lasting effects are attributed to downstream signaling molecules or induced effectors having a long half-life, particularly in specific cell types. Here, we describe a mechanism explaining the long-term effects of IFN-I. Following receptor binding, IFN-I is siloed into endosomal compartments. These intracellular “IFN silos” persist for days and can be visualized by fluorescence and electron microscopy. However, they are largely dormant functionally, due to IFN-I–induced negative regulators. By contrast, in individuals lacking these negative regulators, such as ISG15 or USP18, this siloed IFN-I can continue to signal from within the endosome. This mechanism may underlie the long-term effects of IFN-I therapy and may contribute to the pathophysiology of type I interferonopathies.

type I interferon | endosome | cytokine retention

Type I IFN (IFN-I) is a potent antiviral and inflammatory cytokine, with a relatively short half-life (1). It disappears from the plasma several hours after intramuscular administration (2). Even pegylated IFN-I has a half-life of just 2 d in humans (3). Nevertheless, IFN-I has long-term functional effects. For example, expression of *OAS1*, an IFN-stimulated gene (ISG), remains close to peak levels for 1 wk in humans given pegylated IFN-I (4). Similarly, following influenza infection and resolution in mice, bone marrow leukocytes express antiviral genes and are resistant to influenza infection despite lack of detection of IFN-I in the bone marrow or serum on enzyme-linked immunosorbent assay (5). Likewise, individuals lacking ISG15 or USP18, both key negative regulators of IFN-I, have high levels of ISGs in peripheral blood mononuclear cells (PBMCs), as expected, but circulating IFN-I is only detectable in half of ISG15-deficient individuals (6), highlighting the potency of IFN-I. Here, we explore the cellular mechanisms governing this human phenotype.

Results/Discussion

Only half of ISG15-deficient patients have detectable circulating IFN-I, but all display high levels of ISGs in their PBMCs (6), a feature common in all type I interferonopathies (7). We investigated this phenomenon by quantifying ISG messenger RNA (mRNA) after 12 h of priming with IFN-I and 36 h of rest, in hTert-immortalized fibroblasts. At the end of this 48-h period, ISG mRNA levels were significantly higher in ISG15- and USP18-deficient cells than control cells (Fig. 1A). These high ISG mRNA levels persisted up to 5 d after IFN-I priming (mostly, therefore, in absence of cytokine) in ISG15-deficient cells, but returned to prepriming values in control cells after 24 h (8). Given the persistence of ISGs for several days after removal of IFN-I, we investigated whether ISGs accumulated due to a lack of down-regulation during the initial IFN-I exposure or due to active transcription after the cytokine was withdrawn. RT-qPCR on nascent RNA transcripts isolated 36 h to 60 h after the removal of IFN-I revealed active transcription of

ISGs in ISG15- and USP18-deficient cells, but not control cells (Fig. 1B). Thus, transcription occurs long after the elimination of IFN-I in ISG15- and USP18-deficient cells.

We investigated molecules acting farther upstream and detected pSTAT1 and pSTAT2 (mediators of IFN-I proximal signaling) (9) in ISG15- and USP18-deficient cells, but not control cells (Fig. 1C), consistent with transcriptional initiation. Immunofluorescence (IF) staining for total STAT2 at this time point confirmed its nuclear localization (Fig. 1D). In the presence of Cerdulatinib, a Janus kinase (JAK) inhibitor, pSTAT1 and pSTAT2 were abolished, indicating the JAKs were still active 36 h after IFN-I removal (Fig. 1E). We ensured no infinitesimally small amount of residual soluble cytokine was causing this late transcription, by incubating cells with an anti-IFN-I antibody (Fig. 1F and G), and confirmed IFN-I was not being transcribed in the cells (Fig. 1H). We did detect minute amounts of IFN-I in the supernatant, but it was completely blocked by the IFN-I antibody (Fig. 1I). Together, these results demonstrate that IFN-I–mediated signaling can occur in the absence of soluble cytokine.

These results imply either that there is “cytokineless” signaling or that cytokine is present within the cells. We tested these hypotheses by performing volumetric fluorescence imaging after treatment with fluorescently labeled IFN-I. HeLa cells were stimulated with IFN-I for 17 h, washed, rested for 25 h, then imaged by lattice light sheet microscopy (LLSM). We detected IFN-I colocalized with Rab5, an early endosomal marker, demonstrating that IFN-I was being retained in what we call “IFN silos” (Fig. 2A), previously unappreciated sites of IFN-I storage. We detected these silos in all genetic backgrounds (Fig. 2B). While IFN-I receptor (IFNAR) is known to undergo endocytosis (10), this is documentation that IFN-I was present endosomally after signaling cessation. We demonstrate that IFNAR is required for the formation of active IFN-I silos (Fig. 2C). Using single molecule array (SiMoA) (Fig. 2D) and electron microscopy (EM), we confirmed IFN-I intracellular retention (Fig. 2E). Finally, while an endocytosis inhibitor minimally affected proximal signaling, it completely reversed the phenotype in cells lacking negative regulation (Fig. 2F).

The data presented here help resolve the paradox of the long-lasting effects of a cytokine after it is no longer detectable. This phenomenon is explained by the retention of IFN-I in Rab5⁺ endosomes after signaling, with the continuation of signaling largely prevented by USP18 in wild-type cells. Thus, signaling is abolished not by elimination of the cytokine but by the action of negative regulators. The relationship between the turnover of USP18 and the

Author contributions: J.B.A., C.N.G., J.P., and D.B. designed research; J.B.A., J.T., T.W., and M.H. performed research; J.P. contributed new reagents/analytic tools; J.B.A., J.T., T.W., C.N.G., M.H., and D.B. analyzed data; and J.B.A. and D.B. wrote the paper.

The authors declare no competing interest.

This open access article is distributed under [Creative Commons Attribution-NonCommercial-NoDerivatives License 4.0 \(CC BY-NC-ND\)](https://creativecommons.org/licenses/by-nc-nd/4.0/).

¹To whom correspondence may be addressed. Email: dusan.bogunovic@mssm.edu.

First published July 14, 2020.

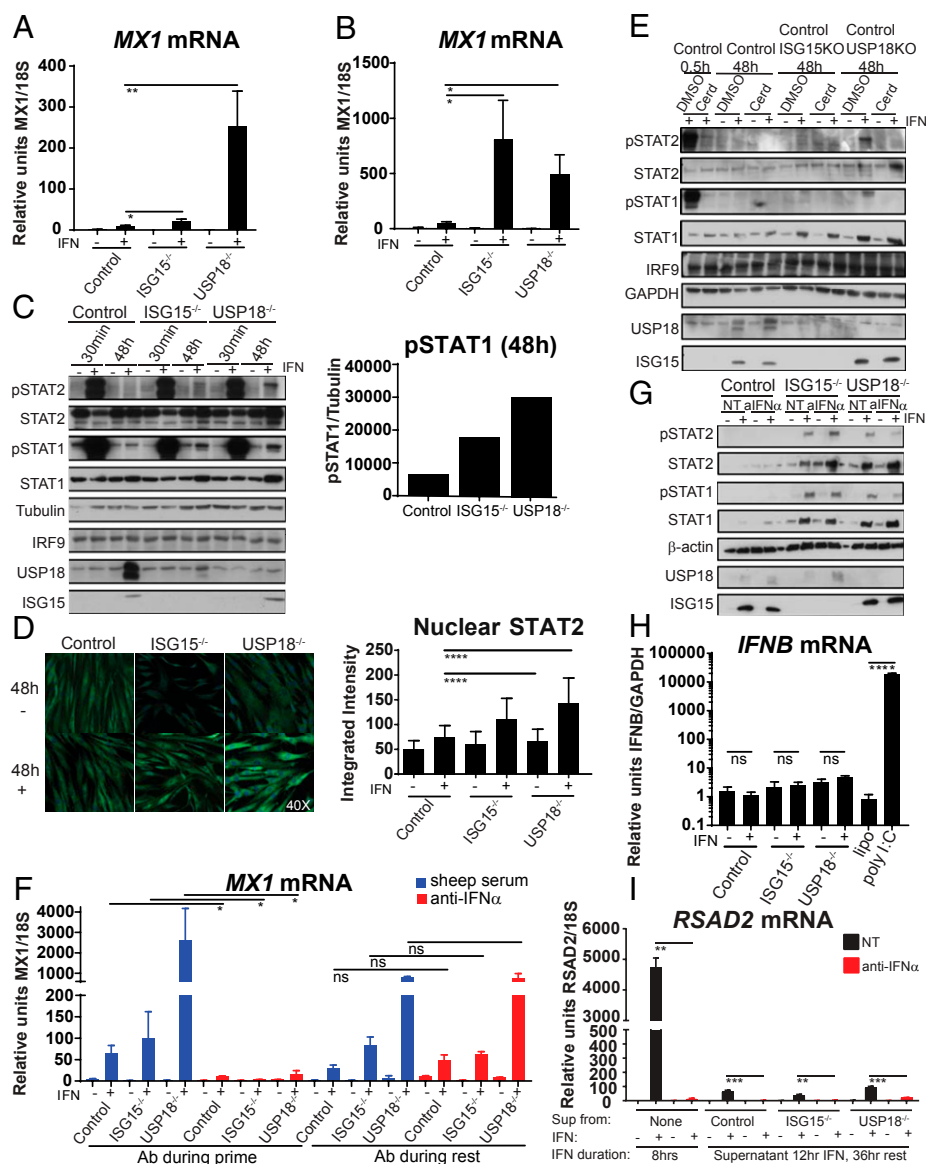


Fig. 1. Persistence of IFN-I signaling in ISG15- and USP18-deficient cells. (A) Control, ISG15-, or USP18-deficient fibroblasts were given 0.197 nM (1,000 u/mL) IFN α 2b for 12 h, washed, and rested for 36 h in all experiments. Relative units of MX1 mRNA was quantified by qPCR. (B) Following A, EU was added for 24 h, RNA containing EU isolated (nascent RNA), and qPCR performed. (C and D) Western blotting or IF for phospho-STAT1, phospho-STAT2, and total STAT2 as per A. Band densitometry of pSTAT1 relative to tubulin for C. (Magnification in D: 40 \times .) (E) Cells were incubated with 10 μ M Cerdulatinib (Cerd) or vehicle (dimethyl sulfoxide [DMSO]) for 4 h following A, and Western blotting was performed. (F and G) Cells were primed and rested with antibodies present, and (F) qPCR or (G) Western blotting was performed. (H) qPCR for *IFNB* mRNA after prime-rest protocol or polyinosinic:polycytidylic acid (poly I:C). (I) Cells were prime-rested as per A, and supernatants were placed on naive control cells for 8 h (NT) or with anti-IFN α . Control cells given 0.197 nM IFN-I (8 h) served as a positive control, and *RSAD2* mRNA was quantified. SEM represented, unpaired Student *t* tests: **P* < 0.05, ***P* < 0.01, ****P* < 0.001, *****P* < 0.0001. ns = not significant.

rate of IFN-I degradation in the endosome may leave room for low levels of IFN-I signaling, in some cell types, potentially accounting for the long-term effects of IFN-I therapy in vivo. It will be of great interest to determine whether endosomal retention of IFN-I contributes to inflammation in diseases for which IFN-I signatures are a prominent feature, such as systemic lupus erythematosus (11), in which the cytokine may not be readily detected, but ISGs are.

Materials and Methods

Cells were hTert-immortalized dermal fibroblasts from control, ISG15-, and USP18-deficient patients. RT-qPCR was performed as previously described (8). For nascent RNA capture, ethynyl uridine (EU) was incubated for 24 h. The mRNA containing EU was isolated for RT-qPCR (12). Western blotting was performed as previously described (8). For confocal microscopy,

cells were stained for DAPI and STAT2 (sc-476; 1:100). Leica SP5 DMI microscope and Cell Profiler were used for analyses. For IFN-I blocking, anti-human IFN α antibody (PBL 31110-1) was used at 0.2 μ g/mL, with sheep serum (Millipore S3772, 1:3 for equivalent concentration) as vehicle. Site-specific labeling of IFN was performed as previously described (13, 14). For fluorescence microscopy, cells were calcium phosphate transfected with pSEMS Rab5 mNeonGreen (pSEMS-26m Covalys), and treated with DY647-IFN α 2 for 17 h, washed, and rested for 25 h. Live-cell imaging was performed by LLSM (15). For EM, cells were stimulated with 0.5 nM biotinylated IFN-I for 15 min or 12 h, then incubated with an anti-IFN α antibody or vehicle for 36 h. For SiMoA, IFN-I primed-rested lysates were run on a SiMoA HD-1 or SR-X.

Data Availability. All supporting data are included in the manuscript.

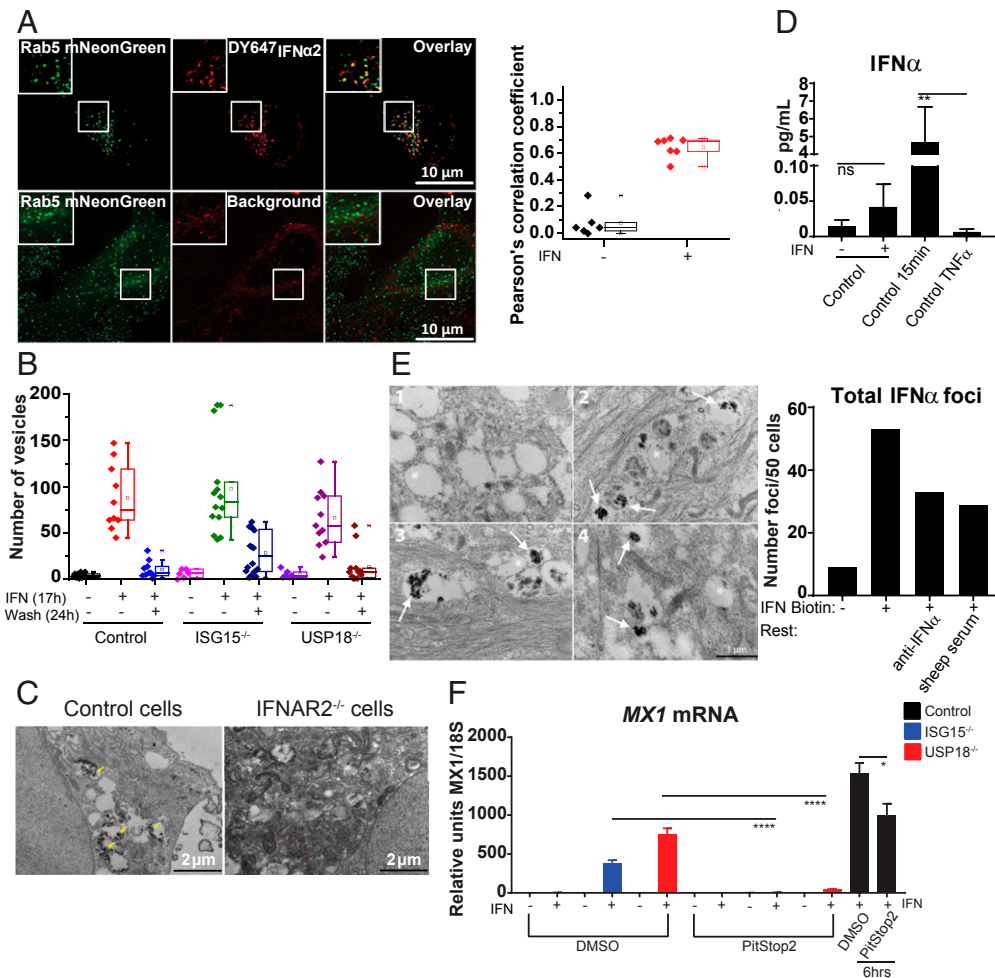


Fig. 2. IFN-I is retained intracellularly. (A) HeLa cells expressing Rab5-mNeonGreen (green) incubated with 5 nM ^{DY647}IFN α 2 (magenta) for 17 h, washed, rested for 25 h, and visualized by LLSM (Top). Untreated cells show background autofluorescence (Bottom). Z projections are of five sections (0.52- μ m total thickness). Box plot shows correlation coefficients for colocalization of IFN α 2 and Rab5 ($n = 10$ cells). (B) Control, ISG15⁻, and USP18-deficient cells were given ^{DY647}IFN α 2 for 17 h and imaged, or rested for 24 h and IFN-I vesicles quantified. (C) EM of Control or IFNAR2-deficient cells given 0.5 nM of IFN-I biotin for 15 min. Yellow arrows denote positive immunoreactivity. (D) Prime-rested cells evaluated by SiMoA, $P = 0.0093$. (E) EM of control cells given 0.5 nM of IFN-I biotin for 12 h, washed and rested in media containing 0.2 μ g/mL anti-IFN α or vehicle (sheep serum) for 36 h. Representative example of (1) negative control without IFN-I biotin; (2) IFN-I biotin 12 h, 36 h rest; (3) IFN-I biotin 12 h, anti-IFN α during 36 h rest; and (4) IFN-I biotin 12 h, sheep serum during 36 h rest. Asterisk denotes unlabeled endosome; arrow denotes positive immunoreactivity within endosome; $n = 50$ cells per condition. (F) Cells were primed-rested in DMSO or 100 μ M PitStop2, and qPCR was performed. Cells given IFN-I with DMSO or PitStop2 for 6 h served as controls. SEM represented, unpaired Student t tests: * $P < 0.05$, **** $P < 0.0001$.

ACKNOWLEDGMENTS. We thank Allison Sowa and Bill Janssen from the Mount Sinai Microscopy Core and Ludovic Debure and Dr. Thomas Wisniewski at New York University for their assistance with SiMoA (Grants AG08051 and R01AF058267). Funding sources are as follows: Deutsche

Forschungsgemeinschaft to J.P. (Grants PI 405/10 and PI 405/14), National Institute of Allergy and Infectious Diseases to D.B. (Grant R01AI127372), and Virus-Host Interactions training grant to J.B.A. (Grant 5T32AI007647-17).

1. E. C. Borden *et al.*, Interferons at age 50: Past, current and future impact on biomedicine. *Nat. Rev. Drug Discov.* **6**, 975–990 (2007).
2. Y. Shechter, L. Preciado-Patt, G. Schreiber, M. Fridkin, Prolonging the half-life of human interferon-alpha 2 in circulation: Design, preparation, and analysis of (2-sulfo-9-fluorenylmethoxycarbonyl)-interferon-alpha 2. *Proc. Natl. Acad. Sci. U.S.A.* **98**, 1212–1217 (2001).
3. B. J. Brennan, Z. X. Xu, J. F. Grippo, Evaluation of the absolute bioavailability of pegylated interferon alfa-2a after subcutaneous administration to healthy male volunteers: An open-label, randomized, parallel-group study. *Clin. Ther.* **34**, 1883–1891 (2012).
4. L. Lai, C. K. Hui, N. Leung, G. K. Lau, Pegylated interferon alpha-2a (40 kDa) in the treatment of chronic hepatitis B. *Int. J. Nanomedicine* **1**, 255–262 (2006).
5. T. Hermesh, B. Moltedo, T. M. Moran, C. B. López, Antiviral instruction of bone marrow leukocytes during respiratory viral infections. *Cell Host Microbe* **7**, 343–353 (2010).
6. X. Zhang *et al.*, Human intracellular ISG15 prevents interferon- α/β over-amplification and auto-inflammation. *Nature* **517**, 89–93 (2015).
7. J. Taft, D. Bogunovic, The Goldilocks zone of type I IFNs: Lessons from human genetics. *J. Immunol.* **201**, 3479–3485 (2018).
8. S. D. Speer *et al.*, ISG15 deficiency and increased viral resistance in humans but not mice. *Nat. Commun.* **7**, 11496 (2016).
9. C. Schindler, D. E. Levy, T. Decker, JAK-STAT signaling: From interferons to cytokines. *J. Biol. Chem.* **282**, 20059–20063 (2007).
10. D. Chmiest *et al.*, Spatiotemporal control of interferon-induced JAK/STAT signalling and gene transcription by the retromer complex. *Nat. Commun.* **7**, 13476 (2016).
11. M. P. Rodero, Y. J. Crow, Type I interferon-mediated monogenic autoinflammation: The type I interferonopathies, a conceptual overview. *J. Exp. Med.* **213**, 2527–2538 (2016).
12. K. Helenius *et al.*, Requirement of FTHIH kinase subunit Mat1 for RNA Pol II C-terminal domain Ser5 phosphorylation, transcription and mRNA turnover. *Nucleic Acids Res.* **39**, 5025–5035 (2011).
13. D. A. Jaitin *et al.*, Inquiring into the differential action of interferons (IFNs): An IFN-alpha2 mutant with enhanced affinity to IFNAR1 is functionally similar to IFN-beta. *Mol. Cell. Biol.* **26**, 1888–1897 (2006).
14. S. Waichman *et al.*, Functional immobilization and patterning of proteins by an enzymatic transfer reaction. *Anal. Chem.* **82**, 1478–1485 (2010).
15. B. C. Chen *et al.*, Lattice light-sheet microscopy: Imaging molecules to embryos at high spatiotemporal resolution. *Science* **346**, 1257998 (2014).